Experimental Entanglement Activation from Discord in a Programmable Quantum Measurement

Gerardo Adesso,[1] Vincenzo D'Ambrosio,[2] Eleonora Nagali,[2] Marco Piani,[3] and Fabio Sciarrino[2]

[1]*School of Mathematical Sciences, University of Nottingham, University Park, Nottingham NG7 2RD, United Kingdom*
[2]*Dipartimento di Fisica, Sapienza Universitá di Roma, Roma 00185, Italy*
[3]*Institute for Quantum Computing and Department of Physics and Astronomy,*
University of Waterloo, Waterloo N2L 3G1, Canada

In quantum mechanics, observing is not a passive act. Consider a system of two quantum particles A and B: if a measurement apparatus M is used to make an observation on B, the overall state of the system AB will typically be altered. When this happens, no matter which local measurement is performed, the two objects A and B are revealed to possess peculiar correlations known as quantum discord. Here, we demonstrate experimentally that the very act of local observation gives rise to an activation protocol which converts discord into distillable entanglement, a stronger and more useful form of quantum correlations, between the apparatus M and the composite system AB. We adopt a flexible two-photon setup to realize a three-qubit system (A, B, M) with programmable degrees of initial correlations, measurement interaction, and characterization processes. Our experiment demonstrates the fundamental mechanism underpinning the ubiquitous act of observing the quantum world and establishes the potential of discord in entanglement generation.

The revolution brought in by quantum mechanics has required a deep change in the way we think about physics and about nature itself. At the same time, it has led to the development of disruptive technologies and, in recent years, to the birth of quantum information processing [1]. Of the many ways in which quantum physics differs from classical one, two are especially striking: the measurement process leads almost always to some disturbance, and nonclassical correlations—including but not reducing to quantum entanglement [2]—can exist between separate physical systems.

These two key signatures of departure from classicality are deeply connected. To appreciate this, let us briefly review the model of measurement depicted by von Neumann [3]. A complete measurement on a quantum system B in a orthonormal basis $|n\rangle_B$ can be realized by letting B interact with a measurement apparatus M, initialized in a fiducial pure state $|0\rangle_M$, through a controlled unitary V_{BM} such that $V_{BM}|n\rangle_B|0\rangle_M = |n\rangle_B|n\rangle_M$. The measurement would then be accomplished by a readout of M. Let us consider the more general situation where B is only a part of a composite system, its complement being denoted by A, and let us indicate with $\chi_{A|B}$ the initial state of the AB system. Just before the readout, the premeasurement state

$$\rho_{AB|M} = (\mathbb{I}_A \otimes V_{BM})(\chi_{A|B} \otimes |0\rangle\langle 0|_M)(\mathbb{I}_A \otimes V_{BM}^\dagger) \quad (1)$$

will typically display quantum entanglement [2] between the apparatus M and the AB system. It is natural to wonder: when is the creation of entanglement between locally measured systems and apparatus (un)avoidable?

The answer is intertwined with the concept of quantum discord [4,5], a nonclassical signature in composite systems which corresponds to the amount of correlations between two or more parties necessarily destroyed during a minimally disturbing local measurement, and similarly quantifies the minimal informational disturbance induced on the system by such a measurement [4]. Quantum discord, as a representative of a general type of nonclassical correlations [6], has received widespread attention both for its fundamental role in defining the border between the classical and quantum world [7–12], and for its possible resource power for information processing and quantum computation, even in absence of entanglement [13–24]. This power, however, has not been fully demonstrated to date [6,25,26].

In Refs. [8,9], a general result was proven: there exists only a special class of states of AB for which one can measure B in some basis $|n\rangle_B$ without inducing disturbance, and such that no entanglement is generated between M and AB in the premeasurement stage. These are the quantum-classical states with zero discord (from the perspective of B), taking the form $\varpi_{A|B} = \sum_n p_n \tau_A^n \otimes |n\rangle\langle n|_B$, where p_n is a probability distribution and each τ_A^n is a density operator for A. For any other state $\chi_{A|B}$, its amount of quantum discord determines the minimum entanglement which is activated, i.e., necessarily established with the apparatus M during a local probing of B. This was theoretically established in [8,9], leading to the proposal to quantify discord exactly in terms of the minimum activable entanglement (see also [27,28] for alternative schemes). Depending on how the created entanglement is quantified, measuring discord via activation may coincide with other approaches [6], e.g., related to distances from the set of quantum-classical states [29,30].

The observation of the predicted qualitative and quantitative correspondence between discord and generated entanglement is the main focus of this Letter. Besides the foundational relevance, the fact that entanglement is necessarily generated during a measurement renders discord useful in schemes aimed at producing entanglement for quantum technological applications [8,31,32]. It is worth mentioning that, once system-apparatus entanglement is generated in the activation framework thanks to initial discord between subsystems A and B, such entanglement can be used flexibly, and, in particular, be mapped into $A|B$ entanglement via local operations and classical communication [31].

We demonstrate experimentally the entanglement activation from discord by realizing a programmable quantum measurement process with bulk optics, see Fig. 1. We consider a family of initial states $\chi_{A|B}$ of two qubits AB with variable degree of discord, and we use a third logical qubit M (as the apparatus) to perform a variety of local measurements on B. Taken *prima facie*, the verification of the results of [8,9] would require to implement a continuous set of measurements, which is impossible in practice. We develop a rigorous procedure to define a discrete net of settings which reliably approximates a continuous sampling over the Bloch sphere of B, see Fig. 2. This novel approach is reminiscent of the notion of ϵ-net for metric spaces [33,34] and tackles the problem of considering a worst case scenario over a continuous set, at variance with other experiments where only average values are cared for [35] or polynomial interpolation is invoked [36]. Based on a finite set of data, we conclude that as soon as the initial state $\chi_{A|B}$ is nonclassically correlated, entanglement is activated for any possible measurement setting. The minimum amount of entanglement activated, over all possible local measurements, agrees quantitatively with the suitably quantified initial amount of discord, verifying the theoretical predictions [8,9,31,37]. Furthermore, when the initial state $\chi_{A|B}$ is itself entangled, genuine tripartite entanglement is detected among A, B, and M in the premeasurement state $\rho_{AB|M}$ [37] by means of a witness operator [38]. Our Letter puts quantum discord on the firm ground of an operational ingredient for entanglement generation.

Activation protocol: description and implementation.— The experimental implementation of the activation protocol is based on a two-qubit system AB encoded in the polarization states of two photons "A" and "BM", and an ancillary qubit M corresponding to the two possible paths that photon BM can take. The protocol is divided in three stages, see Fig. 1.

Generation: By exploiting spontaneous parametric down conversion in a nonlinear crystal, we generate two polarization maximally entangled photons in the Bell singlet state $|\Psi^-\rangle_{A|B}$, with $|\Psi^\pm\rangle_{A|B} = \frac{1}{\sqrt{2}}(|H\rangle_A|V\rangle_B \pm |V\rangle_A|H\rangle_B)$, where (H,V) are linear horizontal and vertical polarization, respectively [39]. In order to complete the Bell basis, the three other Bell states $|\Psi^+\rangle_{A|B}$ and $|\Phi^\pm\rangle_{A|B} = \frac{1}{\sqrt{2}}(|H\rangle_A|H\rangle_B \pm |V\rangle_A|V\rangle_B)$ are generated by applying to
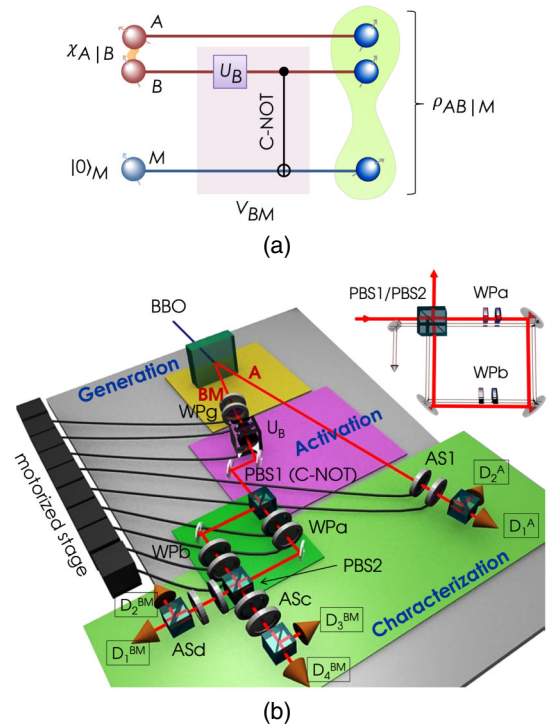

FIG. 1 (color online). Activation protocol: design and experimental setup. (a) Circuit model for the activation protocol [8,9,37]. The initial discord of the state $\chi_{A|B}$ is activated into distillable entanglement for the state $\rho_{AB|M}$ by a local variable operation (V_{BM}) composed by a single qubit operation on B (U_B) and a C-NOT between B and M. (b) Experimental setup. Two polarization entangled photons are generated in a beta barium borate crystal (BBO) via spontaneous parametric down conversion [39]. The entangled state is changed in different Bell states by adopting birefringent wave plates (WPg). The U_B is realized by two wave plates [40] while the C-NOT is realized by the polarizing beam splitter (PBS1) which couples polarization and path of photon BM. To characterize the output state, we adopt wave plates WPa, WPb, and analysis stages ASc, ASd, and AS1. Finally, single-photon detectors (D_i^A, D_j^{BM}) measure photon coincidences. All the WPs are mounted on motorized stages controlled via computer. The inset displays the equivalent displaced Sagnac interferometric scheme adopted in the experiment [41–43].

$|\Psi^-\rangle_{A|B}$ a suitable combination of local unitary Pauli operators $\{\sigma_i\}$, implemented by exploiting the effect of birefringent wave plates on photon BM (WPg in Fig. 1). Thus, a generic Bell diagonal mixed state $\chi_{A|B}$ can be obtained by switching between different Bell states for an appropriate time depending on the weight of the corresponding state in the statistical mixture [45].

Activation: The activation procedure for the state $\chi_{A|B}$ consists of two steps. The interaction V_{BM} is realized by first applying a variable unitary operation U_B to system B, which plays the role of selecting the measurement basis $|n\rangle_B$, i.e., the observable to be measured. Up to irrelevant phases, the basis $|n\rangle_B$ is uniquely defined by a Bloch vector $\vec{n}$ [40]. Then B interacts with the apparatus M via a C-NOT gate, see Fig. 1(a). After these local operations, the initial
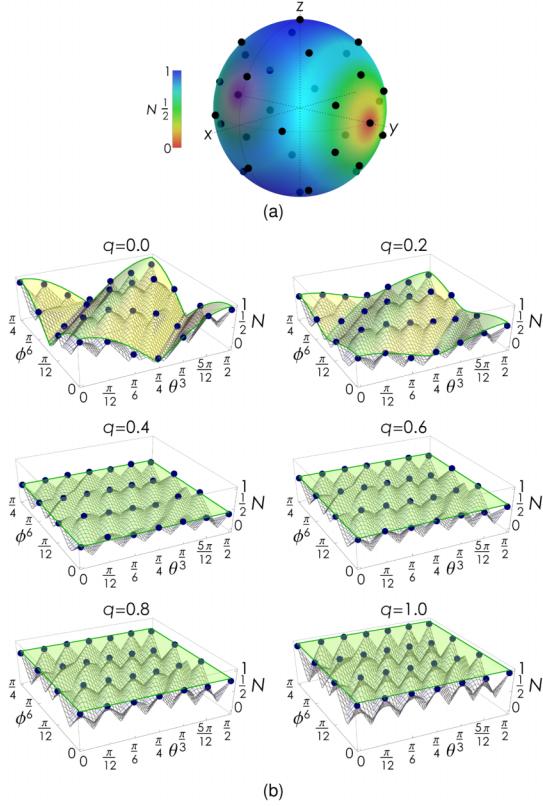
FIG. 2 (color online).   Activation protocol: experimental results.
(a) Measurement bases for qubit B defined by Bloch vectors
$\pm\vec{n}(\theta_j,\phi_k)$ (dots), where θ, ϕ are wave plates angles [40]; the
Bloch sphere is overlaid with a density plot of the expected
negativity of the output premeasurement state $N(\rho_{AB|M}^{(q,\theta,\phi)})$ for
$q = 0$. (b) Comparative results of the activation protocol. Each
plot corresponds to a different value of q, and within each panel, 28
different settings are varied for U_B. Each blue point amounts to the
entanglement $N(\rho_{AB|M}^{(q,\theta_j,\phi_k)})$ of the corresponding premeasurement
state reconstructed by tomography; the errors, evaluated from the
Poissonian statistics of photon events, are below 10^{-2}. In each plot,
we include the lower bound $N_{\mathrm{low}}(\rho_{AB|M}^{(q,\theta,\phi)})$ on the negativity derived
in Eq. (B.5) of [44] (wireframe meshed surface), which remains
positive for $q > 0$ confirming that we sampled enough settings for
U_B to certify the unavoidable entanglement creation from initial
discord. The green translucent smooth surfaces correspond to
theoretical expectations $N_{\mathrm{th}}(\rho_{AB|M}^{(q,\theta,\phi)})$ [44].

discord of the state $\chi_{A|B}$ is activated into distillable
entanglement in the state $\rho_{AB|M}$. Experimentally, the
operation U_B on the polarization of photon BM is imple-
mented by the two wave plates U_B in Fig. 1; the C-NOT
gate is achieved by exploiting a polarizing beam splitter
(PBS1) which implements the following transformation:
$|H\rangle_B|a\rangle_M \rightarrow |H\rangle_B|a\rangle_M$ and $|V\rangle_B|a\rangle_M \rightarrow |V\rangle_B|b\rangle_M$, where
the path states $\{|a\rangle_M, |b\rangle_M\}$ define the computational basis
for the logical qubit M.

Characterization: To measure the activated entangle-
ment, we fully reconstruct the output premeasurement

state $\rho_{AB|M}$ via quantum state tomography [46], requiring
projective measurements over polarization of both photons
and the path of photon BM. While polarization measure-
ment for photon A is easily performed with two wave
plates and a PBS (AS1), photon BM requires a more
complex setup based on an interferometer which is shown
in Fig. 1. In each arm of the interferometer, a quarter-wave
plate and a half-wave plate are exploited to measure
polarization of photon BM; depending on this measure-
ment, the photon will leave PBS2 from exit c or exit d.
Then the polarization state of photon BM depends only on
its path inside the interferometer; hence, a polarization
analysis stage (ASc and ASd) is sufficient to perform a
measurement of qubit M. Instead of the Mach-Zehnder
interferometer of Fig. 1, in the experiment, we adopted a
more compact and stable displaced Sagnac interferometer
[41–43], see inset of Fig. 1(b). Both photons are finally
collected by single-mode fibers and sent to single-photon
detectors; see also [44].

The activation protocol does not need destructive mea-
surements; hence, the generated entanglement can be used
for further processing. In our experimental setup, the
entanglement is activated after PBS1 which implements
a C-NOT gate between polarization and path of photon BM.
As an alternative approach, one could encode qubits A, B,
and M in three different photons or other physical systems
like trapped ions or superconducting qubits. The destruc-
tive measurements are performed here only in order to
verify the activation process.

Experimental state preparation and characterization.—
Following the above procedure, we prepared the qubits A
and B in a family of symmetric Bell diagonal states of the
form

$$\chi_{A|B}^{(q)} = q|\Psi^+\rangle\langle\Psi^+|_{A|B} + \frac{1-q}{2}(|\Phi^+\rangle\langle\Phi^+|_{A|B} + |\Psi^-\rangle\langle\Psi^-|_{A|B}).$$

$$(2)$$

Here, the parameter $q \in [0, 1]$ regulates the quantumness of
correlations in the initial state $\chi_{A|B}^{(q)}$: for $q = 0$, the state is
only classically correlated, for any $q > 0$, it has discord,
while for $q > 1/2$, the state is further entangled. The
activation theorem predicts that for any $q > 0$, the pre-
measurement state $\rho_{AB|M}^{(q,U_B)}$ is entangled for all possible
choices of U_B. The minimum entanglement in the pre-
measurement state over all choices of U_B, measured, e.g.,
by the negativity N [2,47], defines a measure of discord
for the initial state known as negativity of quantumness
[8,30,48], $Q_N(\chi_{A|B}^{(q)}) = \min_{U_B} N(\rho_{AB|M}^{(q,U_B)})$. When B is a
qubit, like in our case, the negativity of quantumness
coincides with an independently defined geometric mea-
sure of discord $D(\chi_{A|B})$ given by the trace distance between
$\chi_{A|B}$ and the closest quantum-classical state $\varpi_{A|B}$ [30,49]
(see Appendix). In particular, for the class of states in

Eq. (2), the trace-distance discord reads $D(\chi_{A|B}^{(q)}) = q$ while their initial entanglement measured by the negativity [2,47] is $N(\chi_{A|B}^{(q)}) = \max(0, 2q - 1)$.

In the experiment, we pick six evenly spaced representative values for q. The operator U_B is implemented through a combination of a quarter-wave plate and a half-wave plate whose optical axes are rotated, respectively, by θ and ϕ with respect to the direction of linear horizontal polarization, which overall amounts to measuring B in a Bloch direction $\pm\vec{n}(\theta, \phi)$ [40]. We define a discrete net of values (θ_j, ϕ_k), which provides an adequate sampling—reminiscent of the notion of ϵ-net for metric spaces [33,34]—of the Bloch sphere for the purpose of entanglement activation, see [44] for the mathematical details. This procedure brings us down to measure $N(\rho_{AB|M}^{(q,\theta_j,\phi_k)})$ in 28 different settings (j, k) for any chosen value of q, defined by the wave plates angles (θ_j, ϕ_k) with $\theta_j = j(\pi/12)$, $\phi_k = k(\pi/12)$, $j = 0, \ldots, 6$, $k = 0, \ldots, 3$. The corresponding Bloch directions $\pm\vec{n}(\theta_j, \phi_k)$ are displayed in Fig. 2(a) [40]. The wave plates angles are programmed by a computer-controlled motorized stage as illustrated in Fig. 1(b). An example of tomographically reconstructed state is reported in [44].

Demonstration of entanglement activation.—The activation results are shown in Fig. 2(b) together with the closely matching theoretical surface based on Eq. (A.1) of [44] which considers an ideal implementation of the state in Eq. (2). We observe a satisfactory agreement with the experimental acquisitions which confirms our high degree of control on all stages of the experiment. Notice how the case $q = 0$, where the initial state $\chi_{A|B}$ of Eq. (2) has zero discord, is the only case in which for certain values of U_B, the apparatus M does not necessarily entangle with the observed system AB, in accordance with the theoretical formulation of the activation protocol [8,9].

We complete our plots with a grid of lower bounds to $N(\rho_{AB|M}^{(q,\theta,\phi)})$ for arbitrary θ, ϕ. The bounds, which originate from purposely derived continuity limits for the negativity [44], allow us to infer—based on the finite net of experimental data—that for $q > 0$, the premeasurement state will always display entanglement between M and the AB for all possible measurement choices on B, hence providing a sound verification of the activation theorem [8,9]. Only in the case $q = 0$, when the initial state $\chi_{A|B}$ of Eq. (2) has zero discord, we find that for certain measurement settings $N(\rho_{AB|M}^{(0,\theta_j,\phi_k)})$ is essentially vanishing within the experimental imperfections. The output entanglement was generally found to be minimized by $\theta_j = \pi/4$, $\phi_k = 0$; while for $q > 1/3$, any choice of U_B produces the same entanglement in the premeasurement state apart from experimental fluctuations, see Fig. 2(b).

We can now exploit our data to verify the quantitative prediction of the activation theorem [8,9], as shown in Fig. 3(a). We find experimentally that the minimum output

entanglement $\min_{j,k} N(\rho_{AB|M}^{(q,\theta_j,\phi_k)})$ generated with the apparatus, measured by negativity, precisely matches the amount of trace-distance discord $D(\chi_{A|B}^{(q)})$ initially detected between A and B [44]. This demonstrates the operational power of discord as "entanglement potential" [8,9,16] and proves successfully the activation of distillable bipartite entanglement from input discord. Small discrepancies (of at most 0.1 units) from the theoretical green line can be traced back to imperfections in the initial preparation of the four polarization Bell states of photons A and BM, which in our implementation reach a mean purity of $(93.6 \pm 0.2)\%$, consistent, e.g., with the experimental value for $D(\chi_{A|B}^{(q=1)})$.

Finally, in case the initial state $\chi_{A|B}^{(q)}$ is entangled as well, we observe that genuine tripartite entanglement is created in the premeasurement state among A, B, and M as a result of the activation protocol [37]. This is verified by detecting suitable entanglement witnesses [2,38] for input and output states [44] as presented in Fig. 3(b). Theoretically, the expectation values for both witnesses on the corresponding states should coincide and be given by $(1/2) - q$ (solid green line); we find a satisfactory agreement between the two data sets and the theory, detecting, in particular, negative expectation values for the two witnesses in the relevant parameter range $q > 1/2$.

Conclusions.—The experimental observation of the activation protocol, presented as an abstract theorem in [8,9], brings the notion of quantumness in composite systems to a more concrete level than ever before. Our demonstration establishes the usefulness of various forms of nonclassical correlations as resources for information
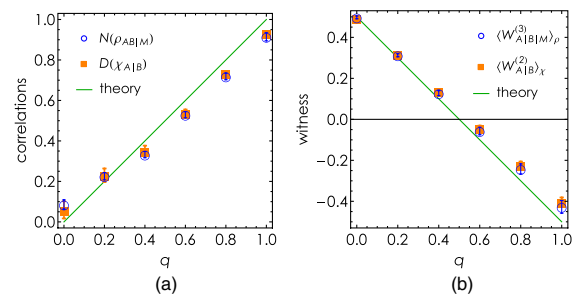

FIG. 3 (color online). Activation protocol: quantitative verification. (a) The minimum output entanglement activated with the apparatus, measured by the negativity $\min_{(\theta,\phi)} N(\rho_{AB|M}^{(q,\theta,\phi)})$, is verified to match the input discord $D(\chi_{A|B}^{(q)})$ in the system, measured by the trace distance from the set of quantum-classical states. (b) Input bipartite entanglement activates into genuine tripartite entanglement [37]. Measured expectation values of two witness operators (negative values detect entanglement) [2,38] are plotted; $W_{A|B}^{(2)}$ is a witness for bipartite entanglement in the initial state $\chi_{A|B}^{(q)}$, while $W_{A|B|M}^{(3)}$ is a witness for genuine tripartite Greenberger-Horne-Zeilinger–type entanglement among A, B, and M in the premeasurement state $\rho_{AB|M}^{(q)}$ [44].

processing: discord is necessarily activated into bipartite entanglement, and bipartite entanglement into genuine tripartite entanglement, by the act of performing a local measurement. We believe an approach based on an ϵ-net construction such as ours can effectively be adopted in future experiments aimed at substantiating mathematical predictions via sampling continuously distributed parameters, in particular, in worst case scenarios. The implementation of a von Neumann chain [3,37] may be further considered, exploiting recent advances in integrated quantum photonics [50–52]. We hope our Letter can stimulate further endeavours towards a deeper physical understanding and practical exploitation of quantumness, in its manifold manifestations, for information processing and communication.

Appendix: Measures of correlations.—The negativity, a measure of entanglement for a bipartite state $\chi_{A|B}$, can be defined as $N(\chi_{A|B}) = \|\varrho_{A|B}^\Gamma\|_1 - 1$, where the suffix Γ denotes partial transposition [2], and $\|O\|_1 = \mathrm{Tr}\sqrt{O^\dagger O}$ is the trace norm, i.e., the sum of the singular values of O. The negativity of quantumness, a measure of discord, can be defined in terms of the activation framework of Fig. 1(a) [8,9,30,31,37] as $Q_N(\chi_{A|B}) = \min_{U_B} N(\rho_{AB|M}^{(U_B)})$ (notice that the entanglement in the premeasurement states $\rho_{AB|M}^{(U_B)}$ is always distillable [8,9]). The trace-distance discord $D(\chi_{A|B})$ is defined as the minimum distance, in trace norm, between $\chi_{A|B}$ and the set of quantum-classical states $\varpi_{A|B} = \sum_n p_n \tau_A^n \otimes |n\rangle\langle n|_B$, namely $D(\chi_{A|B}) = \min_{\varpi_{A|B}} \|\chi_{A|B} - \varpi_{A|B}\|_1$ [30,49]. If B is a qubit, then $Q_N(\chi_{A|B}) = D(\chi_{A|B})$ as first proven in [30]. We observe this equivalence experimentally in Fig. 3(a).

[1] M. A. Nielsen and I. L. Chuang, *Quantum Computation and Quantum Information* (Cambridge University Press, Cambridge, 2010).

[2] R. Horodecki, P. Horodecki, M. Horodecki, and K. Horodecki, Rev. Mod. Phys. **81**, 865 (2009).

[3] J. von Neumann, *Mathematical Foundation of Quantum Mechanics* (Princeton University Press, Princeton, 1955).

[4] H. Ollivier and W. H. Zurek, Phys. Rev. Lett. **88**, 017901 (2001).

[5] L. Henderson and V. Vedral, J. Phys. A. **34**, 6899 (2001).

[6] K. Modi, A. Brodutch, H. Cable, T. Paterek, and V. Vedral, Rev. Mod. Phys. **84**, 1655 (2012).

[7] W. H. Zurek, Rev. Mod. Phys. **75**, 715 (2003).

[8] M. Piani, S. Gharibian, G. Adesso, J. Calsamiglia, P. Horodecki, and A. Winter, Phys. Rev. Lett. **106**, 220403 (2011).

[9] A. Streltsov, H. Kampermann, and D. Bruss, Phys. Rev. Lett. **106**, 160401 (2011).

[10] D. Girolami, T. Tufarelli, and G. Adesso, Phys. Rev. Lett. **110**, 240402 (2013).

[11] A. Streltsov, and W. H. Zurek, Phys. Rev. Lett. **111**, 040401 (2013).

[12] F. G. S. L. Brandão, M. Piani, and P. Horodecki, arXiv:1310.8640.

[13] A. Datta, A. Shaji, and C. M. Caves, Phys. Rev. Lett. **100**, 050502 (2008).

[14] B. P. Lanyon, M. Barbieri, M. P. Almeida, and A. G. White, Phys. Rev. Lett. **101**, 200501 (2008).

[15] B. Eastin, arXiv:1006.4402.

[16] R. Chaves and F. de Melo, Phys. Rev. A **84**, 022324 (2011).

[17] D. Cavalcanti, L. Aolita, S. Boixo, K. Modi, M. Piani, and A. Winter, Phys. Rev. A **83**, 032324 (2011).

[18] M. Gu, H. M. Chrzanowski, S. M. Assad, T. Symul, K. Modi, T. C. Ralph, V. Vedral, and P. Koy Lam, Nat. Phys. **8**, 671 (2012).

[19] B. Dakic *et al.*, Nat. Phys. **8**, 666 (2012).

[20] A. Streltsov, H. Kampermann, and D. Bruss, Phys. Rev. Lett. **108**, 250501 (2012).

[21] T. K. Chuan, J. Maillard, K. Modi, T. Paterek, M. Paternostro, and M. Piani, Phys. Rev. Lett. **109**, 070501 (2012).

[22] A. Fedrizzi, M. Zuppardo, G. Gillett, M. Broome, M. Almeida, M. Paternostro, A. White, and T. Paterek, Phys. Rev. Lett. **111**, 230504 (2013).

[23] D. Girolami *et al.*, arXiv:1309.1472.

[24] Z. Merali, Nature (London) **474**, 24 (2011).

[25] P. Horodecki, J. Tuziemski, P. Mazurek, and R. Horodecki, arXiv:1306.4938.

[26] G. L. Giorgi, Phys. Rev. A **88**, 022315 (2013).

[27] L. Mazzola and M. Paternostro, Sci. Rep. **1**, 199 (2011).

[28] A. Farace, F. Ciccarello, R. Fazio, and V. Giovannetti, Phys. Rev. A **89**, 022335 (2014).

[29] K. Modi, T. Paterek, W. Son, V. Vedral, and M. Williamson, Phys. Rev. Lett. **104**, 080501 (2010).

[30] T. Nakano, M. Piani, and G. Adesso, Phys. Rev. A **88**, 012117 (2013).

[31] S. Gharibian, M. Piani, G. Adesso, J. Calsamiglia, and P. Horodecki, Int. J. Quantum. Inform. **09**, 1701 (2011).

[32] P. J. Coles, Phys. Rev. A **86**, 062334 (2012).

[33] W. A. Sutherland, *Introduction to Metric and Topological Spaces* (Oxford University Press, Oxford, 1975).

[34] P. Hayden, D. Leung, P. W. Shor, and A. Winter, Commun. Math. Phys. **250**, 371 (2004).

[35] J. Emerson, M. Silva, O. Moussa, C. Ryan, M. Laforest, J. Baugh, D. G. Cory, and R. Laflamme, Science **317**, 1893 (2007).

[36] M. Lobino, D. Korystov, C. Kupchak, E. Figueroa, B. C. Sanders, and A. I. Lvovsky, Science **322**, 563 (2008).

[37] M. Piani and G. Adesso, Phys. Rev. A **85**, 040301(R) (2012).

[38] O. Gühne and G. Toth, Phys. Rep. **474**, 1 (2009).

[39] P. G. Kwiat, K. Mattle, H. Weinfurter, A. Zeilinger, A. V. Sergienko, and Y. Shih, Phys. Rev. Lett. **75**, 4337 (1995).

[40] The operator U_B is decomposed as a sequence of two rotated wave plates, $U_B = R^T(\phi)U_B^H R(\phi)R^T(\theta)U_B^Q R(\theta)$, where $U_B^H = \text{diag}(1, -1)$ and $U_B^Q = \text{diag}(1, i)$ correspond to a half- and a quarter-wave plate, respectively (with optical axes parallel to the horizontal polarization), and

$$R(\alpha) = \begin{pmatrix} \cos\alpha & -\sin\alpha \\ \sin\alpha & \cos\alpha \end{pmatrix}$$

is a rotation. The measurement interaction resulting from applying a C-NOT gate after U_B is equivalent (up to local unitaries) to the one achieving $V_{BM}|n\rangle_B|a\rangle_M = |n\rangle_B|n\rangle_M$, where $|n\rangle_B = U_B^\dagger|H\rangle_B$ is a state with Bloch vector $\vec{n}(\theta, \phi) = \{-\cos[2(\theta - 2\phi)]\sin(2\theta), -\sin[2(\theta - 2\phi)], \cos[2(\theta - 2\phi)]\cos(2\theta)\}$. Correspondingly, $U_B^\dagger|V\rangle_B$ has Bloch vector $-\vec{n}(\theta, \phi)$. By periodicity, we can restrict to a parameter range $\theta \in [0, \pi/2]$, $\phi \in [0, \pi/4]$, so that the basis vectors $\pm\vec{n}(\theta, \phi)$ cover the whole Bloch sphere of qubit B.

[41] E. Nagali, S. Felicetti, P.-L. de Assis, V. D'Ambrosio, R. Filip, and F. Sciarrino, Sci. Rep. **2**, 443 (2012).

[42] S. P. Walborn, P. H. Souto Ribeiro, L. Davidovich, F. Mintert, and A. Buchleitner, Nature (London) **440**, 1022 (2006).

[43] R. Okamoto, J. L. O'Brien, H. F. Hofmann, and S. Takeuchi, Proc. Natl. Acad. Sci. U.S.A. **108**, 10067 (2011).

[44] See Supplemental Material at http://link.aps.org/supplemental/10.1103/PhysRevLett.112.140501 for additional details on the experimental and theoretical procedures; this includes Refs. [53–55].

[45] J. Lavoie, R. Kaltenbaek, M. Piani, and K. J. Resch, Phys. Rev. Lett. **105**, 130501 (2010).

[46] D. F. V. James, P. G. Kwiat, W. J. Munro, and A. G. White, Phys. Rev. A **64**, 052312 (2001).

[47] G. Vidal and R. F. Werner, Phys. Rev. A **65**, 032314 (2002).

[48] I. A. Silva, D. Girolami, R. Auccaise, R. Sarthour, I. Oliveira, T. Bonagamba, E. deAzevedo, D. Soares-Pinto, and G. Adesso, Phys. Rev. Lett. **110**, 140501 (2013).

[49] F. M. Paula, T. R. de Oliveira, and M. S. Sarandy, Phys. Rev. A **87**, 064101 (2013).

[50] A. Politi, M. J. Cryan, J. G. Rarity, S. Y. Yu, and J. L. O'Brien, Science **320**, 646 (2008).

[51] A. Crespi, R. Ramponi, R. Osellame, L. Sansoni, I. Bongioanni, F. Sciarrino, G. Vallone, and P. Mataloni, Nat. Commun. **2**, 566 (2011).

[52] A. Crespi, R. Osellame, R. Ramponi, D. J. Brod, E. F. Galvão, N. Spagnolo, C. Vitelli, E. Maiorino, P. Mataloni, and F. Sciarrino, Nat. Photonics **7**, 545 (2013).

[53] V. Buzek, M. Hillery, and R. F. Werner, Phys. Rev. A **60**, R2626 (1999).

[54] F. De Martini, V. Buzek, F. Sciarrino, and C. Sias, Nature (London) **419**, 815 (2002).

[55] F. Ciccarello, T. Tufarelli, and V. Giovannetti, New J. Phys. **16**, 013038 (2014).